

SUPERCARGING: A METHOD FOR IMPROVING PATCH-CLAMP PERFORMANCE

CLAY M. ARMSTRONG AND ROBERT H. CHOW

Department of Physiology, University of Pennsylvania, Philadelphia, Pennsylvania 19104

ABSTRACT Patch-clamp performance can be improved without altering the normal headstage configuration described by (Hamill, O. P., A. Marty, E. Neher, B. Sakmann, and F. J. Sigworth, 1981, *Pfluegers Arch. Eur. J. Physiol.*, 391:85–100). The “supercharging” method permits resolution of such fast events as calcium and sodium tail currents. Digital computer modeling and analog electronic simulation were used to identify appropriate shapes for the command voltage and the voltage applied to a capacitor tied to the input of the headstage. The voltage command pulse consists of a step with a brief (5–15 μ s) rectangular spike on its leading edge. Spike amplitude is a function of the membrane capacitance and the access resistance. The spike drives current through the access resistance and speeds charging of the membrane capacitance, making it possible to complete a voltage step within 5–15 μ s. Clamping speed is independent of the electrode and feedback resistance over a wide range. The second function of the patch clamp amplifier is current measurement, and good time resolution requires suppression of the capacity transient. This can be accomplished by applying an appropriately shaped voltage to the small capacitor tied to the input of the headstage. Series resistance compensation for ionic current transients does not interfere with supercharging. Although the focus of this paper is on whole cell recording, the supercharging concept may prove useful for single channel and bilayer recording techniques.

This paper describes a simple method for improving the performance of a patch clamp. The method is useful for both whole cell and single channel experiments, and has four major advantages. (a) A voltage step can be imposed on the membrane in 5 μ s or less. (b) Clamping speed is independent of electrode and feedback resistance over a wide range. (c) The rather tedious adjustments usually required for nulling the capacity transient are simplified. (d) Ionic current can be measured beginning 5–15 μ s after the initiation of a step.

This method uses the normal head stage configuration described by Hamill et al. (1981) and illustrated in Fig. 1, but alters the command voltage and the voltage applied to the “ballistic charging capacitor,” C_b . Because in a real experiment it is difficult or impossible to measure V_m and V_- directly, the responses of this system were simulated on a digital computer, and subsequently confirmed by trials with a patch-clamp head stage connected to a dummy membrane. The equations for the simulations were as follows (symbols are identified in Fig. 1):

$$dV_0/dt = \omega_a(V_c - V_-) \quad (1)$$

$$I = (V_0 - V_c)/R_f \quad (2)$$

$$dV_m/dt = (V_{el} - V_m)/R_{a2} C_m \quad (3)$$

$$dV_-/dt = f_1(f_2 V_- + V_0/R_f + V_{el}/R_{a1} + C_b dV_b/dt + \omega_a C_f V_c) \quad (4)$$

$$dV_{el}/dt = (V_- - V_{el})/(R_{a1} C_{el}) - (V_{el} - V_m)/(R_{a2} C_{el}). \quad (5)$$

I is the membrane current. The factors in Eq. 4 are:

$$f_1 = 1/(C_f + C_b + C_{in})$$

$$f_2 = \omega_a C_f - 1/R_f - 1/R_{a1}.$$

Eq. 1 describes the behavior of an operational amplifier with gain-bandwidth product of ω_a (cf. Sigworth, 1983). R_{a1} and R_{a2} (see below) are components of the access resistance, which is the net resistance between the amplifier's inverting input and the membrane. The access resistance is often higher than the electrode resistance in free solution.

COMPUTER SIMULATIONS WITH LOW FEEDBACK RESISTANCE

Fig. 2A shows the simulated response to a square command step (V_c) with the parameters listed in the figure legend. The amplifier characteristics match those of the OPA-111 (Burr Brown Research Corporation, Tucson, AZ). The feedback resistance of the amplifier is 10 M Ω , the value that we use for whole cell clamping. This low resistance improves the frequency response for monitoring current at the expense of some increase in noise. C_{el} was assumed to be negligible for these simulations.

The simulations show that current supplied by the amplifier output forces V_- to follow V_c with fair accuracy,

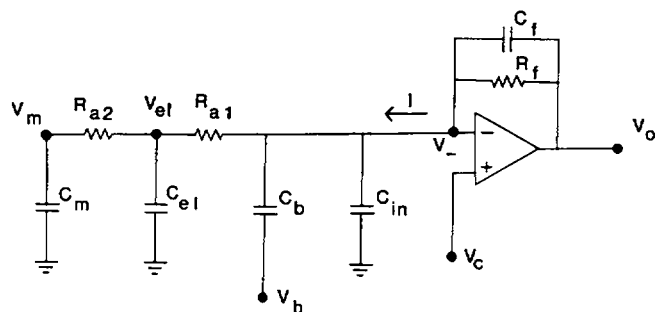


FIGURE 1 Schematic of the patch clamp headstage.

but there is a rounding when V_- reaches $\sim 90\%$ of its final value. The current that drives up V_- flows largely through C_f . A high value of C_f thus improves clamping performance, but worsens the time resolution of current measurement. Current through R_a charges the membrane capacitance, and V_m has an (approximately) exponential time course, with a time constant of $R_a C_m$. I (the current) is seen to rise to a peak in $\sim 12 \mu\text{s}$, and it then decays with a time course that depends on both the rate of rise of V_m and the time constant $R_f C_f$, requiring $132 \mu\text{s}$ to fall to 1 nA .

V_m can be made to change more rapidly if V_- is made larger during the charging phase (cf. Goldman and Morad, 1977). Fig. 2 *B* shows the response when the command step

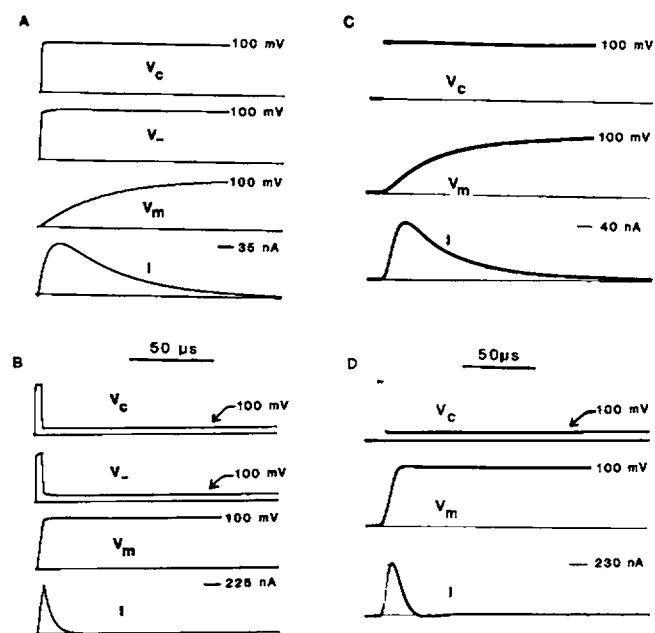


FIGURE 2 Clamp responses when feedback resistance is low. *A* and *B* are computer simulations. *C* and *D*, which are checks on the accuracy of the computer simulations, were recorded from a patch clamp head stage attached to a model membrane. (*A*) Responses to a square step command with $R_f = 10 \text{ M}\Omega$, $C_f = 0.5 \text{ pF}$, $R_{a1} + R_{a2} = 2 \text{ M}\Omega$, $C_m = 18 \text{ pF}$, $C_e = C_b = 0$, $V_b = 0$. (*B*) Same parameters as in *A*, but the command step has a spike on its leading edge. Note the faster response of V_m and I . (*C*) Head stage responses to a square step command with the same parameters as in *A* and *B*. (*D*) Head stage responses to a command step with a spike on its leading edge, with the same parameters.

has a large spike of $5 \mu\text{s}$ duration on its leading edge. V_m now rises very rapidly and is within 5% of its final level at the end of the spike. I rises until the spike terminates, and then decays with a time constant of $\sim 5 \mu\text{s}$ (the product of $R_f C_f$), falling to 1 nA in $32 \mu\text{s}$. Clearly the simulated responses of V_m and I are improved by the initial spike on the command voltage. A method for approximating the proper spike size is described below.

Further simulations (not illustrated) show that an increase in the access resistance can be compensated for by increasing the amplitude of the spike, with no degradation in clamp speed. In theory access resistance can be increased to the point that causes amplifier saturation without detriment to performance.

VERIFICATION OF COMPUTER SIMULATION WITH A MODEL MEMBRANE

The accuracy of the simulations was confirmed by applying the voltage patterns of Fig. 2, *A* and *B*, to a head stage made with an OPA 111 amplifier and configured according to the diagram of Fig. 1. To observe V_m directly, we connected a follower to the point labeled V_m in Fig. 1. This is, of course, not possible in a real experiment. The input capacitance of the follower increases the apparent membrane capacitance, and we took this into account in reckoning the "membrane capacitance." V_- was not measured directly. Fig. 2 *C* shows the result of applying a square step voltage command, with R_f equal to $10 \text{ M}\Omega$, $R_{a1} + R_{a2} = 2 \text{ M}\Omega$, and $C_m = 18 \text{ pF}$. These values approximate an experiment on a very large isolated cell with an average patch pipette. C_f was purely stray capacitance, which we estimated to be 0.5 pF . The traces of V_m and I closely resemble those of the simulation shown in Fig. 2 *A*. When an initial spike is added to the command potential (Fig. 2 *D*), V_m rises much more rapidly, and the time course of the I transient is also much quicker. In general, the computer simulations seem to agree closely with the experiment using a headstage and a model membrane.

ELECTRODE CAPACITANCE AND BALLISTIC CHARGING

Patch-clamp experiments are complicated by the presence of an electrode capacitance (Fig. 1) that can distort the current transient. We have found that electrode capacitance can be modeled adequately as a lumped capacitance, as in Fig. 1. Realistic values are R_{a1} $0.5 \text{ M}\Omega$, R_{a2} $2 \text{ M}\Omega$, and C_e 2.5 pF . The adverse effects of C_e are ameliorated by application of a shaped voltage, V_b , to the ballistic charging capacitor, C_b . The purpose is to supply most of the current for charging C_m and C_e through C_b rather than from the amplifier output: the membrane thus is charged ballistically rather than by feedback.

The results of this procedure are shown in Fig. 3. V_c has an initial spike as in the preceding illustrations. V_b also has a spike, slightly rounded, on its leading edge, that serves to

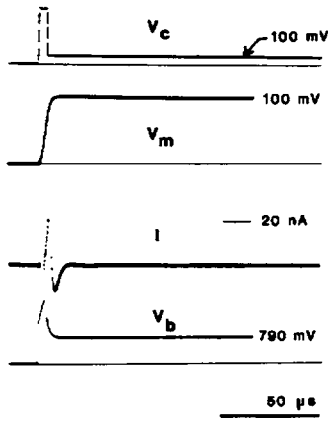


FIGURE 3 Head stage responses when electrode capacitance is included. The command step has a spike on its leading edge. A shaped voltage, V_b , is simultaneously applied to the ballistic capacitor, C_b , to reduce the capacity current transient, which is smaller than in Fig. 1 despite the presence of finite electrode capacitance. Dashed connecting lines have been added to the oscilloscope traces for clarity. $R_f = 10 \text{ M}\Omega$, $C_f = 0.5 \text{ pF}$, $R_{a1} = 0.5 \text{ M}\Omega$, $R_{a2} = 2.0 \text{ M}\Omega$, $C_{el} = 2.5 \text{ pF}$, $C_m = 11.17 \text{ pF}$, $C_b = 2.1 \text{ pF}$.

charge C_{el} to a voltage near to V_- during the command spike, and then discharge it at the end of the strike. Overall, the effect is to make the voltage across C_{el} follow V_- while drawing little current from the amplifier output. After the spike, V_b returns to a steady level that can be calculated from the formula

$$\Delta V_{b \text{ final}} = \Delta V_{c \text{ final}}(C_m + C_{el} + C_{in} + C_b)/C_b, \quad (6)$$

where the deltas indicate the change from the initial value. V_m changes very quickly, and is within a few percent of the required value in $5 \mu\text{s}$. The current is a multiphasic transient that dies out after $\sim 15 \mu\text{s}$. Thus valid measures of ionic current can begin after $15 \mu\text{s}$ or, since the transient is linear, earlier if a method for subtraction of linear capacity current, e.g., the P/4 procedure (Bezánilla and Armstrong, 1977), is used.

Tests have also been performed using compensation for the access resistance. We find that supercharging does not alter the behavior of the clamp when compensation is applied. Slight slowing of the compensating signal that is fed back (using a 10- or 20- μs time constant) makes it possible to compensate for 80 or even 100% of the access resistance without producing steady-state oscillations. The clamp, however, shows a pronounced tendency to ring under these circumstances. Ringing at the onset of a step can be prevented by cancellation of the capacity transient, with or without supercharging. We have chosen not to include an illustration using series resistance compensation, for although the ringing can be suppressed, this does not alter the fact that the response to a current change is a damped oscillation, leading to distortion of any ionic current being measured. High access resistance combined with large current leads to an error in the imposed mem-

brane voltage. This is a limitation of the patch-clamp technique, whether supercharging is used or not.

DETERMINATION OF SPIKE AMPLITUDE

Were it not for C_{el} , spike amplitude for optimal charging of the capacitance could be approximated (for a 5- μs spike) from the formula

$$V_{\text{spike}} = V_{\text{step}}(R_a C_m / 5 \mu\text{s} + 0.5), \quad (7)$$

whenever $R_a C_m$ is large compared with $5 \mu\text{s}$. In practice, when C_{el} is present, we find that the correct command spike can be quickly and accurately determined by increasing spike amplitude until the slow component of the capacity transient, which is related to the charging of C_m , is nulled out. The final value of V_b is next determined from Eq. 6, after measuring the summed capacitance $C_m + C_b + C_{in} + C_{el}$. This can be done very quickly by applying a rectangular step and integrating the capacity current transient. The amplitude of the spike on V_b is then adjusted empirically to minimize whatever capacity transient remains after setting the final value of V_b . It is helpful if the spike on V_b rises and falls exponentially, with a time constant of $\sim 1 \mu\text{s}$. In real experiments, we have found that this time constant need be adjusted only once, and is sufficiently close to optimal on most electrodes that it requires no further alteration. Overall these adjustments are considerably easier than the ones required with conventional patch-clamps, which involve adjusting the amplitude and time constant of two or three exponentials produced by a transient generator.

COMPUTER SIMULATIONS WITH HIGH FEEDBACK RESISTANCE

We have also simulated clamp performance with high feedback resistors, although we have not had the facilities to confirm our findings with a head stage. We simulated the clamping of a cell-attached or excised patch, for which C_m has a very low value, 0.01 pF, corresponding to an area of $\sim 1 \mu\text{m}^2$. Total access resistance is $4.5 \text{ M}\Omega$ (R_{a1} 0.5 M Ω ,

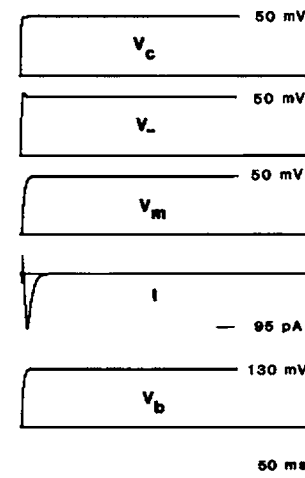


FIGURE 4 Computer simulations with high feedback resistance. Responses to a square command step when $R_f = 10 \text{ G}\Omega$, $C_f = 0.5 \text{ pF}$, $C_m = 1.0 \text{ pF}$, $R_{a1} = 0.5 \text{ M}\Omega$, $R_{a2} = 4.5 \text{ M}\Omega$, $C_{el} = 2.5 \text{ pF}$, $C_m = 0.01 \text{ pF}$, $C_b = 2.1 \text{ pF}$. V_b is depicted in the figure. Note that the current transient has returned to $< 1 \text{ pA}$ within $20 \mu\text{s}$ of imposing the step.

R_{s2} 4.0 M Ω), and we assumed an electrode capacitance of 2.5 pF. The calculations assume that the current signal (I) has been peaked, as it is customary with patch clamps, and that the overall bandwidth is 10 KHz, the bandwidth claimed by some commercial patch-clamps. No spike is necessary at the beginning of the command voltage because C_m is low. V_m reaches 95% of its final value in 6 or 7 μ s. The capacity current transient on I can be effectively nulled by applying a slightly rounded step to C_b . The amplitude of the step is given by Eq. 6, and it is rounded with a time constant of 0.8 μ s. The time constant was adjusted empirically to reduce the capacity current transient. It is seen that after the transient, I has settled back to within the equivalent of 1 pA of its final value (zero) within $\sim 15 \mu$ s.

This method of nulling the transient thus involves only one adjustment, the time constant of V_b , while V_b itself is calculated from Eq. 6. Measurement of channel current

can begin a very short time after the step. The method differs from the usual one mainly in that V_b has a very rapid rise.

Received for publication 28 August 1986 and in final form 18 February 1987.

REFERENCES

- Bezanilla, F., and C. M. Armstrong. 1977. Inactivation of the sodium channel. I. Sodium current experiments. *J. Gen. Physiol.* 70:549-566.
- Goldman, Y., and M. Morad. 1977. Measurement of transmembrane potential and current in cardiac muscle: a new voltage clamp method. *J. Physiol. (Lond.)*. 268:613-654.
- Hamill, O. P., A. Marty, E. Neher, B. Sakmann, and F. J. Sigworth. 1981. Improved patch-clamp techniques for high-resolution current recording from cells and cell-free membrane patches. *Pfluegers Arch. Eur. J. Physiol.* 391:85-100.
- Sigworth, F. J. 1983. Electronic design of the patch clamp. In *Single-Channel Recording*. B. Sakmann and E. Neher, editors. Plenum Publishing Corp., New York. 3-35.